HOKKAIDO UNIVERSITY

Title	SHEAR CAPACITY OF REINFORCED HIGH-STRENGTH CONCRETE BEAMS WITHOUT WEB REINFORCEMENT
Author(s)	S. V. T. J. PERERA; MUTSUYOSHI, H.
Description	The Thirteenth East Asia-Pacific Conference on Structural Engineering and Construction (EASEC-13), September 11-13, 2013, Sapporo, Japan.
Relation	Proceedings of the Thirteenth East Asia-Pacific Conference on Structural Engineering and Construction (EASEC-13), September 11-13, 2013, Sapporo, Japan, B-6-4.
Citation	Proceedings of the Thirteenth East Asia-Pacific Conference on Structural Engineering and Construction (EASEC-13), B-6-4
Issue Date	2013-09-11
Doc URL	https://hdl.handle.net/2115/54265
Type	conference paper
File Information	easec13-B-6-4.pdf

Hokkaido University Collection of Scholarly and Academic Papers

Hokkaido University Collection of Scholarly and Academic Papers : HUSCAP

SHEAR CAPACITY OF REINFORCED HIGH-STRENGTH CONCRETE BEAMS WITHOUT WEB REINFORCEMENT

S.V.T.J. PERERA[1*†] and H. MUTSUYOSHI[1]

[1]*Department of Civil and Environmental Engineering, Saitama University, Japan*

ABSTRACT

Three series of reinforced concrete (RC) beams without web reinforcement were tested to determine their diagonal cracking shear strengths and ultimate shear capacities. Within each series, the shear span to depth ratio was held constant at 3.0, 3.5, or 4.0 while the characteristic compressive strength of concrete was varied from 36 to 194 MPa in otherwise identical specimens. Test results indicated that the ratio of uniaxial compressive strength to tensile strength of the concrete was proportional to concrete brittleness. According to the JSCE code and the ACI code, the shear strength of RC beams increases with increasing concrete strength. However, test results showed that, the JSCE code and the ACI code for predicting shear strength were not safe.

Keywords: Diagonal cracking shear strength, ultimate shear capacity, RC beams.

1. INTRODUCTION

The use of high-strength concrete (HSC) is growing faster than applicable design methods are being developed since it enables the use of smaller cross-sections, longer spans, reduction in girder height and improved durability (Mutsuyoshi et al. 2010). However, the diagonal cracking shear strength of HSC beams does not increase as expected with the increase in the compressive strength of concrete (Perera et al. 2009).

The diagonal cracking shear force in reinforced concrete (RC) members is transferred in various ways. After development of flexural cracks, shear force acting on a cracked section is carried by: 1) the shear resistance of un-cracked concrete in the compression zone; 2) the interlocking action of aggregates along the rough concrete surfaces on each side of the crack; and, 3) the dowel action of the longitudinal reinforcement as shown in Fig.1. With the formation of a diagonal crack, a beam without web reinforcement becomes unstable and fails. This type of failure is usually called diagonal tension failure. For rectangular beams, approximately 53-90% of the vertical shear is carried by aggregate interlocking and un-cracked concrete in the compression zone (Taylor and Browm 1963). Meanwhile, if sufficient anchorage length is provided in a RC beam, after a diagonal crack develops, failure occurs due to concrete crushing in the upper end. In this type of failure, the

* Corresponding author: Email: janaka@mail.saitama-u.ac.jp

† Presenter: Email: janaka@mail.saitama-u.ac.jp

load is transferred directly from the loading point to supports owing to arch action. This type of failure is called shear compression failure.

Current specifications in the JSCE and ACI codes for shear strength of RC beams are based on the results of thousands of beam tests using mostly normal-strength concrete (NSC) (JSCE 2002; ACI 2005). Because of the recent use of HSC with a strength exceeding 100MPa, it has become necessary to check the validity of present shear design methods when applied to these higher concrete strengths.

There has been much discussion on the correct relationship between concrete compressive strength (f'_c) and concrete diagonal cracking shear strength and ultimate shear capacity, even for NSC. The current JSCE code assumes that the diagonal cracking shear strength is essentially proportional to $f'^{1/3}_c$ while the ACI has concluded it is proportional to $f'^{0.5}_c$. However, Perera et al. (2009) showed that the diagonal shear capacity of HSC beams does not increase as expected with the increase in the compressive strength of concrete. In addition, the mechanism of shear failure is not fully understood because of the lack of research on HSC beams with different shear span to depth ratios (*a/d* ratios) (Kobayashi et al. 2008). Previous work has shown that the effect of concrete strength on shear strength is also dependent on the *a/d* ratio of the beam (Mphonde and Frantz 1984).

This paper summarizes results of an experimental program that examined the effect of concrete strength and *a/d* ratio on diagonal cracking shear strength and ultimate shear capacity of nine reinforced concrete beams without web reinforcement.

2. EXPERIMENTAL PROGRAM

2.1. Specimen details

The concrete properties of spec are tabulated in Table 1. The type of aggregate was crushed granite with a 2.64 g/cm^3 density, 0.42% absorption, and fineness modulus of 6.64. The properties of steel bars used in the experiment are listed in Table 2.

As tabulated in Table 1, nine identical beams without web reinforcement were used in this study. The cross sections and layout of test beams are shown in Fig. 2. Three high strength steel bars (f_y = 750 MPa) were laid at the bottom of the section so shear failure would precede flexural failure. The test variables were compressive strength of concrete and *a/d* ratio as shown in Table 1.

All specimens including RC beams, compressive strength specimens (Φ100x200mm), splitting tensile strength specimens (Φ150x300mm), and fracture energy specimens (100x100x400mm) were cured up to the loading test age to exclude the effects of drying.

2.2. Instrumentation and measurements

Four-point symmetrical loading with a distance of 300 mm between the loading points was statically applied to all specimens (Fig.2). Vertical deflections at the center, shear span and support

of the RC beams were measured by displacement transducers. Electrical-resistance strain gauges were used to record the strain in concrete at the mid span of the beam. All cracks, which developed during the loading were observed and marked in detail. The test was stopped when crushing of the concrete in compression and considerable loss of load carrying capacity was observed.

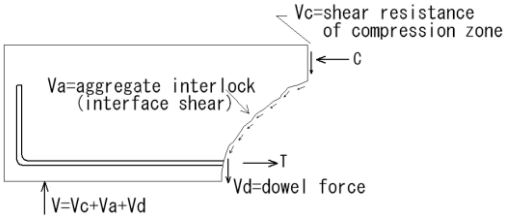

Figure 1: Shear transfer mechanism of slender beams

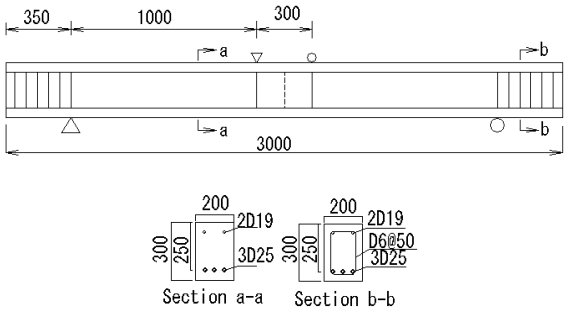

Figure 2: Details of RC beam (unit: mm)

The compressive strength, splitting tensile strength, and fracture energy of concrete were measured on the same day as the RC beam test.

2.3. Brittleness number (*B*)

Various parameters have been proposed to characterize the brittleness of concrete. The characteristic length, $l_{ch}=EG_F/f_t^2$, proposed by Hillerborg (Hillerborg 1985) has been used to characterize the brittleness of concrete, rock and glass. The normalized shear strength v_c/f'_t (v_c: shear strength) of geometrically similar beams, is governed by the dimensionless ratio between absolute structure size (D) and l_{ch} (Gustafsson and Hillerborg 1988). This ratio has been regarded as a measure of the brittleness of structural elements which are sensitive to tensile stress-induced fracture; a higher value of B corresponding to a more brittle structural element.

$$B = \frac{f_t^2 D}{(EG_F)} \tag{1}$$

where; E is Young's modulus (MPa), G_F is fracture energy (N/mm), D is absolute structural element size (mm; in the case of a beam it is equal to effective depth of the beam).

Tensile strength and modulus of elasticity of concrete are dependent on compressive strength, and fracture energy is dependent on aggregate size and compressive strength.

3. RESULTS AND DISCUSSION

3.1. Properties of concrete

The compressive strength, splitting tensile strength, Young's modulus, and fracture energy in concrete at the age of the beam test are tabulated in Table 3. The results show that Young's modulus and fracture energy were 32.1-43.5kN/mm^2 and 0.200-0.250N/mm respectively.

Table 1: Specimen details and test results

Specimen	a/d	f'_c (MPa)	f'_t (MPa)	V_c (kN)	V_u (kN)	Failure mode
NSC-I	3.0	38	3.2	75.0	75.0	DT
NSC-II	3.5	38	3.4	78.0	78.0	DT
NSC-III	4.0	36	3.1	76.5	76.5	DT
HSC-I	3.0	133	6.1	85.5	142.0	SC
HSC-II	3.5	116	5.4	85.0	93.0	SC
HSC-III	4.0	114	5.2	85.0	85.0	DT
HSC-IV	3.0	165	7.4	81.0	226.0	SC
HSC-V	3.5	194	6.8	77.0	80.0	SC
HSC-VI	4.0	183	7.4	75.0	105.5	SC

a/d: Shear span to depth ratio
f'_c: Compressive strength of concrete
f'_t: Splitting tensile strength
V_c: Shear force at diagonal cracking
V_u: Shear force at failure, DT: Diagonal tension failure
SC: Shear compression failure

Table 2: Mechanical properties of steel

Type	f_y (MPa)	E_s (GPa)
D6	360	187
D19	384	200
D25	750	201

f_y: yield strength of steel
E_s: Young's modulus of steel

Table 3: Properties of concrete

Concrete type	E_c (GPa)	G_F (N/mm)	l_{ch} (mm)	f'_c/f_t
NSC-III	32.1	0.200	676	11.6
HSC-III	36.5	0.220	347	21.9
HSC-VI	43.5	0.250	200	24.7

E_c: Young's modulus of concrete
G_F: Fracture energy, l_{ch}: Characteristic length

To analyse the relationship between the brittleness of concrete and concrete strength detail, f'_c/f_t was used. Brittleness number B is proportional to f'_c/f_t as shown in Fig. 3. The value of B and f'_c/f_t increased by 95% and 89% respectively, with increasing concrete strength from 36MPa to 114MPa. Also, B and f'_c/f_t increased by 74% and 13% when concrete strength increased from 114MPa to 183MPa. Therefore, f'_c/f_t can be use as another brittleness measure due to its easy application.

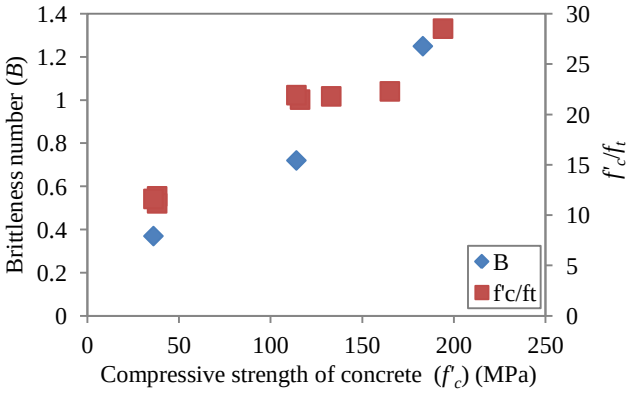

Figure 3: Brittleness of concrete

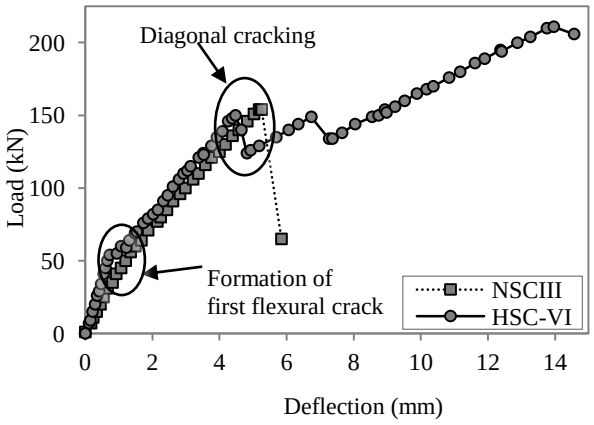

Figure 4: Comparison of load –deflection relationship of RC beams

3.2. Load-deflection behaviour and failure mode

Figure 4 shows the load-deflection curves of tested beams (a/d = 4.0). All beams exhibited similar behavior and beam HSC-VI is described here as an example. In the HSC-VI load-deflection curve, flexural cracks first appeared at an early stage of loading. The load dropped slightly after formation of the first flexural crack, and then continued to rise. The flexural cracking load at which the first

flexural crack formed was 6-57% greater in reinforced HSC beams than NSC beams. This was mainly due to the higher tensile strength of HSC.

A diagonal crack then occurred in the shear span and the load dropped sharply. However, the load soon continued to increase, dropping slightly once again with the formation of another crack. Thus, even though diagonal cracking took place, the beam was still able to bear the applied load through arch action. Finally the beam failed in shear compression when the diagonal cracks in the shear span widened and the concrete near the crack tip in the compression zone was crushed. Beams HSC-I, HSC-II, HSC-IV, HSC-V, and HSC-VI all failed in shear compression while all other beams, including HSC-III, failed in diagonal tension. Diagonal tension failure occurred just after the occurrence of critical diagonal cracking. This failure load is called as diagonal cracking load.

In RC beams with a concrete strength exceeding 100 MPa, when a/d was greater than 3.0, failure occurred after diagonal cracking and the beams failed in shear compression as described above. This failure load is called as ultimate failure load. However, in the case of HSC beams (HSC-III), when a/d was 4.0, diagonal cracking became unstable and the beams failed under diagonal tension. That is, for HSC beams (f'_c > 100 MPa), the transition point between shear compression failure and diagonal tension failure shifted to an a/d greater than 4.0, while for NSC beams it was 3.0 (Kim and Park 1996) (Table 1).

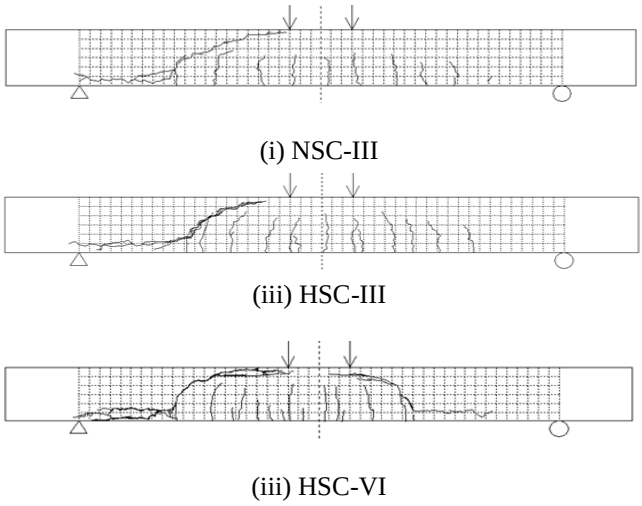

Figure 5: Beam crack pattern (just after failure, a/d=4.0)

3.3. Crack pattern

Figure 5 shows a typical failure crack pattern for RC beams with an a/d=4.0. Vertical flexural cracks initially developed near mid-span. Further loading produced more flexural cracks and also diagonal cracks. As these crack patterns show, the load-carrying mechanism changed significantly as concrete strength changed. At f'_c of 36MPa and 114MPa, the cracks indicated a predominantly flexural behavior. At f'_c of 183MPa, the typical deep beam crack pattern shows the tied-arch behavior with much less vertical flexural cracking.

When f'_c of 36MPa and 114MPa, failure was sudden and occurred soon after inclined cracking. However, at 183MPa, there was significant reserve strength in the beam due to arch action after the crack pattern was fully developed. While inclined cracks formed gradually from a flexural crack for beams with f'_c of 36MPa and 114MPa, in the beams with f'_c of 183MPa it usually developed very suddenly and was often not associated with any particular flexural crack.

At failure, longitudinal splitting along the main reinforcement was prevented in all beams. Observation of the actual failure sequence showed that longitudinal splitting did not initiate the final failure.

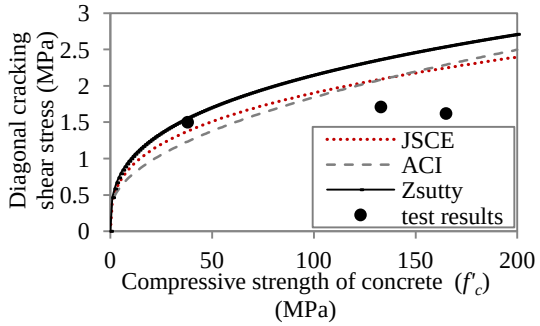

(a) Diagonal cracking shear stress of RC beams (a/d=3.0 series)

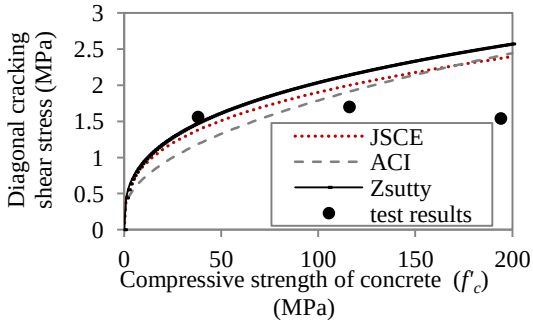

(b) Diagonal cracking shear stress of RC beams (a/d=3.5 series)

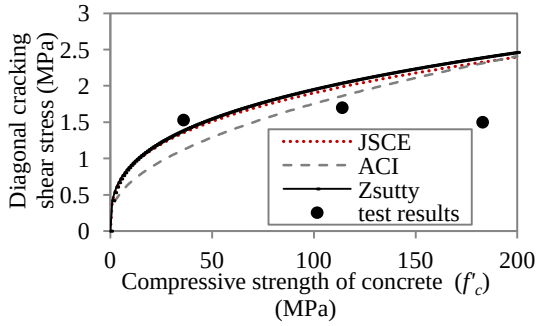

(c) Diagonal cracking shear stress of RC beams (a/d=4.0 series)

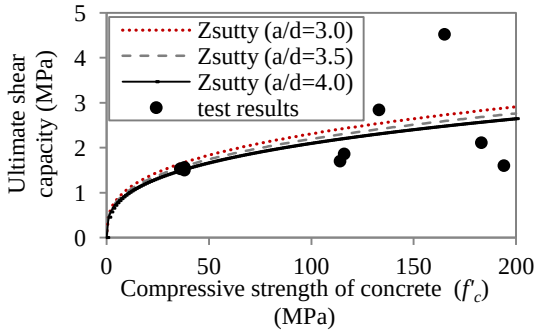

(d) Ultimate shear capacity of RC beams

Figure 6: Shear stress of RC beams

3.4. Prediction of shear behavior

In this study, diagonal cracking shear stress was defined as the shear stress at the time when critical diagonal crack (the crack that caused failure) became inclined and crossed mid-depth.

The results obtained in the tests are compared with values calculated on the basis of the recommendations given in the JSCE code, the ACI code, and equations proposed by Zsutty (JSCE 2002; ACI 2005; Zsutty 1968). All these equations are based on beam tests with relatively low strength concrete.

JSCE code (JSCE 2002):

$$v_c = d^{-1/4}(100\rho_w)^{1/3}\left(0.2f'^{1/3}_c\right) \quad (2)$$

where, v_c is diagonal cracking shear strength, d is effective depth, ρ_w is longitudinal reinforcement ratio, and f'_c is compressive strength of concrete.

ACI Code 308-05 (ACI 2005):

$$v_c = 0.158f'^{1/2}_c + 17.2\rho_w \frac{V_u d}{M_u} \quad (3)$$

where, V_u is shear force at section considered and M_u is bending moment at section considered.

Zsutty equation (Zsutty 1968):

$$v_c = 2.14\left(f'_c \rho_w \frac{d}{a}\right)^{0.333} \quad (4)$$

where, a is shear span.

At ultimate failure

$$v_u = 2.30\left(f'_c \rho_w \frac{d}{a}\right)^{0.333} \quad (5)$$

where, v_u is shear strength at failure.

In the equations by Zsutty (1968) and the JSCE code (2002), the material properties factor in the shear strength of RC beams was evaluated using $f'_c{}^{-1/3}$, unlike the ACI code (2005), which is evaluated using $f'_c{}^{1/2}$.

Fig. 6 presents the measured test results and three predicted values of shear strength expressed in terms of shear stress, from the JSCE code, the ACI code, and Zsutty's statistical analysis of shear strength data (JSCE 2002; ACI 2005; Zsutty 1968). According to the JSCE and the ACI shear prediction equations without limitations, the shear strength of RC beams increases as concrete strength increases (JSCE 2002; ACI 2005). However, the experimental results obtained in this study showed that with increasing concrete strength, the shear strength of HSC beams did not increase.

Table 4: Comparison of experimental results with predicted values of diagonal cracking shear strength and ultimate shear capacity

Specimen	$v_{n,test}/\ v_{n,\ predicted}$			
	Eq. (2) by JSCE	Eq. (3) by ACI	Eq. (4) by Zsutty	Eq. (5) by Zsutty
NSC-I	1.09	1.21	0.96	0.90
NSC-II	1.13	1.32	1.05	0.98
NSC-III	1.11	1.36	1.10	1.02
HSC-I	0.82	0.82	0.72	1.11
HSC-II	0.85	0.90	0.79	0.81
HSC-III	0.85	0.91	0.83	0.78
HSC-IV	0.72	0.71	0.64	1.66
HSC-V	0.65	0.64	0.60	0.58
HSC-VI	0.63	0.65	0.63	0.82
Average	0.87	0.95	0.82	0.96
Standard deviation	0.20	0.28	0.19	0.30

This behavior could be due to smooth fracture surface and high brittleness of the concrete. The smooth fracture surface reduces the aggregate interlock and lowers the diagonal cracking shear strength. Further, the shear resistance of uncracked concrete in the compression zone is lower with HSC as a result of its brittleness. Therefore, for all HSC beams the ACI code and JSCE code over-predicted the shear strength by between 17-58% (JSCE) and 9-57% (ACI) (Table 4).

According to test results, the ultimate shear capacity of HSC beams did not increase with increasing concrete strength. This behavior could be due to high brittleness of the concrete. Also, the predictions by Zsutty on diagonal cracking shear strength and ultimate shear capacity of HSC beams were found to be un-conservative: the averages of the ratio of tested shear strength to

predicted were 0.70 and 0.96 with standard deviations of 0.09 and 0.38 respectively (Fig. 6, Table 4).

All of the above methods were found to be the most reliable for diagonal cracking shear strength predictions of NSC beams (Fig. 6, Table 4). Therefore, further studies on shear behaviour of HSC are recommended.

4. CONCLUSION

This paper summarized the results of an experimental study of shear behavior of reinforced concrete beams without web reinforcement with a nominal concrete strength ranging from 36 to 193MPa. Within the scope of this study, the following conclusions are valid.

HSC beams without web reinforcement showed a very brittle behavior. However, flexural cracking load was 6-57% higher in HSC beams than NSC beams. With increasing concrete strength, the diagonal cracking shear strength did not increase as expected. In the case of HSC beams, when a/d was 4.0, diagonal cracking became unstable and the beams failed in diagonal tension, while for NSC beams it was 3.0. The present JSCE code and ACI code equations for evaluating diagonal cracking shear strength of HSC beams need to be modified.

REFERENCES

ACI committee 318 (2005). Building Code Requirement for Structural Concrete (ACI 318-05) and Commentary (ACI 318R-05), USA.

Gustafsson PJ and Hillerborg A (1988). Sensitivity in Shear Strength of Longitudinal Reinforced Concrete Beams to Fracture Energy of Concrete. ACI Structural Journal, 85-30, May-June 1988, pp. 286-294.

Hillerborg A (1985). Results of Three Comparative Test Series for Determining the Fracture Energy G_F of Concrete. Materials and Structures, Research and Testing (RILEM, Paris), 18-107, Sept.-Oct. 1985, pp. 407-413.

JSCE Guidelines for Concrete No. 3 (2002). Structural Performance Verification, Standard Specification for concrete Structures-2002, Japan.

Kim JK and Park YD (1996). Prediction of Shear Strength of Reinforced Concrete Beams without Web Reinforcement, ACI Material Journal, 98-5, May-June 1996, pp. 213-222.

Kobayashi C, Watanabe K, and Niwa J (2008). Experimental Study on Diagonal Compression Failure of RC Beams using High Strength Concrete, Proceedings of JSCE of 8th International Symposium on Utilization of High Strength and High performance Concrete, Oct. 2008, pp. 1031-1036.

Mphonde AG and Frantz GC (1984). Shear Tests of High- and Low-Strength Concrete Beams without Stirrups, ACI Journal, 81-32, July-August 1984, pp. 350-357.

Mustuyoshi H, Ichinomiya T, Sakurada M, and Perera SVTJ (2010). High-strength concrete for prestressed concrete structures, CPI Trade Journal for the Concrete Industry, August 2010, pp. 42-46.

Perera SVTJ, Quang LH, Mutsuyoshi H, and Minh H (2009). Shear Behavior of Reinforced Concrete Beams Using High-Strength Concrete, Proc. of Japan Concrete Institute (JCI), Vol. 31, No.2, pp. 589-594.

Taylor R and Brown RS (1963). The Effect of the Type of Aggregate on the Diagonal Cracking of Concrete Beams, Magazine of Concrete Research, July 1963.

Zsutty TC (1968). Beam Shear Strength Prediction by Analysis of Existing Data, ACI Journal, 65-11, Nov. 1968, pp. 942-951.